

SOS-Based Generator with 100-kHz Pulse Repetition Frequency ¹

A.V. Ponomarev, S.V. Lozhkin, S.N. Rukin, S.N. Tsyanov, and P.V. Vasiliev

*Institute of Electrophysics Russian Academy of Sciences, Ural Division
106 Amundsen St., Ekaterinburg, 620016, Russia*

Abstract - SOS-based solid-state generator with 100-kHz pulse repetition frequency in burst mode of operation has been developed and experimentally studied. The generator contains low voltage primary capacitive store, step-up pulsed transformer with ferrite core, high voltage pumping capacitor and semiconductor opening switch (SOS diode). The primary capacitive store is switched by ultra-fast IGBT transistor, and energy is transferred to the pumping capacitor via the pulsed transformer in about 1.5 μ s. Current of this process passes via the SOS and insures its forward pumping. After the pulsed transformer ferrite core saturation the current flows through the SOS in reverse direction. The reverse current reaches its maximum value of 200-300 A in about 200 ns. At this instant the SOS cuts off the current in about 5 ns that leads to output pulse formation across external load.

Across external resistive load from 100 Ω to 1 k Ω the generator forms quasi-rectangular pulses with \sim 70-ns FWHM and 20 to 80 kV in amplitude. Maximum peak power is equal to 8.5 MW across the resistive load of 250 - 500 Ohm. The pulse amplitude is within 50 - 60 kV with the pulse energy of about 0.5 J and total efficiency of 70%. In burst mode of operation with 100-kHz PRF the output average power attains 50 kW.

Electrical circuit diagram and principle of the generator operation as well as experimental results obtained are described. The results of numerical simulation of the SOS diode operation are presented also.

1. Introduction

Thanks to the all-solid-state system of energy switching, high-current nanosecond generators equipped with a semiconductor opening switch comprising SOS diodes [1, 2] combine a high pulse repetition rate, stability of output parameters, and a long lifetime. SOS generators operating at various institutions demonstrated their high reliability during applied research work connected with generation of high-current electron beams and high-power X-ray pulses, pumping of gas lasers, ionization of air with a streamer corona

discharge, generation of powerful microwave pulses, etc.

The standard circuitry of a SOS generator includes primary energy storage with a thyristor switch, a magnetic compressor, and a semiconductor opening switch based on SOS diodes. The magnetic compressor is necessary for time compression of energy since the characteristic time of the energy transfer through the thyristor is 10 to 100 μ s, while the pumping time of not longer than 300-400 ns is required for efficient operation of the SOS diode. The energy loss is the largest in the magnetic compressor and the total efficiency of the generator is not over 40-50%.

Moreover, the use of thyristors as primary energy switches limits the maximum pulse repetition frequency of the SOS generator. The time of about 50-100 μ s is required to reliably turn off the thyristor. Considering the charging time of the primary storage, the generator cannot operate at the pulse repetition frequency larger than 5-10 kHz.

The aforementioned drawbacks of the existing circuit design can be eliminated by the following means. On the one hand faster semiconductor devices, which do not take much time for recovery (all-controlled devices), can be used as the primary switch. On the other hand, operating conditions of the SOS diode can be adjusted such as to increase its permissible direct pumping time. In this case, the magnetic compressor unit is omitted from the circuit and the time of the energy transfer from the primary storage corresponds to the time of forward pumping of the opening switch.

This study deals with an attempt to realize this approach. Firstly, fast all-controlled IGBT transistors served as the primary switch with the energy transfer time of 1.5 μ s. Secondly, the pumping regime of the SOS diode was altered, namely the concentration of excess plasma was reduced and its recombination losses were cut down by decreasing the density of the pumping current.

2. Electrical circuit of the generator

A simplified circuit diagram of the generator is shown in Fig. 1. The circuit includes the low-voltage section, which is exposed to air, and the high-voltage section, which is placed in a metal casing filled with

¹ The work was supported in part by Russian Foundation for Basic Researches under Project 05-08-01164

transformer oil. The low-voltage section consists of charging elements: the diode VD1, the inductance coil L1, the primary storage C1, and the primary switch S1. The high-voltage section comprises the step-up pulse transformer PT1, the high-voltage storage C2 (pumping capacitor), the opening switch SOS, and the resistive load R.

The primary storage C1 is made up of 48 capacitors type K78-2 and has the total capacitance of 1.8 μF . The primary switch consists of 10 parallel IGBT transistors type IRG4PH50UD. The charging diode VD1 includes 10 parallel diodes type HFA30PB120. The inductance of the charging coil L1 is 5 μH .

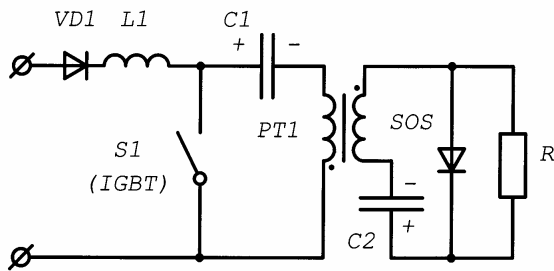


Fig.1. Electrical circuit of the generator.

The pulse transformer PT1 is assembled on four ferritic rings K120 \times 80 \times 12 and has one turn in the primary winding and 40 turns in the secondary winding. The pumping capacitor C2 includes KVI capacitors and has the capacitance of 1 nF. The semiconductor opening switch SOS represents one SOS diode, which contains 280 series-connected semiconductor structures with the surface area of 2 cm^2 . The p-n-junction depth is 180 μm . Every 4 series-connected structures have a copper heat sink measuring 30 \times 30 \times 0.5 mm. Resistors type TVO serve as the load R.

3. Circuit operation and experimental results

The generator is supplied from a DC voltage source containing a three-phase bridge rectifier and a filter capacitor. The initial voltage of the filter is about 540 V. In the resonant regime the primary storage C1 is charged to the voltage of 880-900 V, which corresponds to the stored energy of nearly 0.7 J. The storage charging time is 8 μs . Magnetization of the core of the transformer PT1 is reversed during charging.

When the transistors S1 are turned on, the energy is transferred from C1 to the pumping capacitor C2 through PT1. The charging current of C2 passes in the SOS diode in the forward direction and provides its forward pumping regime. The time of the energy transfer from C1 to C2 is 1.5 μs and corresponds to the forward pumping time of the SOS. The amplitude of the current in the primary switch is as large as 1.5 kA. The forward pumping current of the SOS is 30-35

A (see Fig. 2a). Reverse pumping of the SOS follows the saturation of the transformer PT1 core. The capacitor C2 discharges through the SOS in the reverse direction. The reverse current reaches ~ 240 A in a time interval of about 200 ns. At this moment the current is cut off by the SOS in less than 10 ns, the current is switched to the load, and a nanosecond-long high-voltage pulse is formed at the load (Fig. 2b).

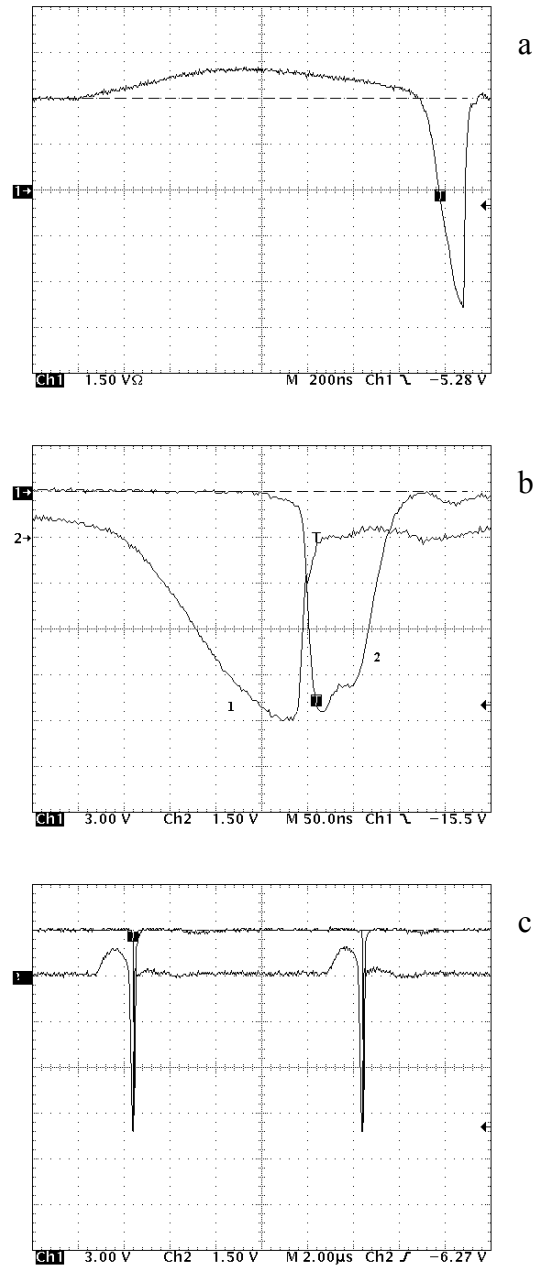


Fig.2. Experimental waveforms: (a) – full current through the SOS diode, 200 ns/div., 53 A/div.; (b) – reverse current through the SOS diode (curve 1), 50 ns/div., 60 A/div., and output voltage pulse across the load $R = 450 \Omega$ (curve 2), 12.5 kV/div.; (c) – waveform of two adjacent pulses of the generator, 2 μs /div.

The capacity of the generator with respect to the pulse repetition frequency was evaluated, load characteristics were measured, and the energy loss in the circuitry elements was estimated in the experiments. The maximum pulse repetition frequency in the pulse burst regime was 100 kHz. It was determined by the charge time of the primary storage (8 μ s) and its discharge time (1.5 μ s). Figure 2c presents an oscillogram of two adjacent current pulses in the SOS and the load voltage at the pulse repetition frequency PRF = 100 kHz. The number of pulses in a burst was determined by adiabatic heating of the circuitry elements and was limited to 10^3 pulses.

Load characteristics of the generator are shown in Fig. 3. As the load resistance increased from 100 to 900 Ohm, the output voltage rose from 20 to 80 kV. The maximum energy and the maximum peak power of the pulse were 0.5 J and 8.5 MW respectively. These values were achieved at the resistance of 270 to 500 Ohm. The FWHM of the pulse was ~ 70 ns over this interval and the average power injected to the load at PRF = 100 kHz was 50 kW.

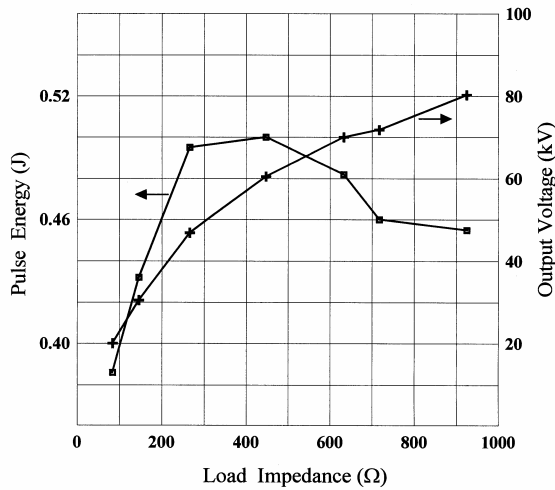


Fig. 3. Load characteristics of the generator.

The total efficiency of the generator was 70% at optimal loads. Most of the energy was lost in two circuitry elements, namely the pulse transformer PT1 (10%) and the SOS (15%). The balance of 5% energy loss was due to the charging circuit and the overvoltage protection circuits of the transistors.

4. Numerical simulation of the SOS diode operation at low current density

Numerical simulation was performed to see specific features of the SOS diode operation at a low current density. The theoretical model described in [3] was used. This model is based on a fundamental system of equations including continuity equations for electrons

and holes and the Poisson equation for the electric field. This system is solved simultaneously with the Kirchhoff equations for electric circuits. The model also takes into account the real doping profile of semiconductor structures.

Calculations revealed specific features of the plasma dynamics in the structure at a low current density at the stages of pumping and current cutoff. As distinct from the classical regime of the SOS effect, which is realized at current densities equal to units of kA/cm^2 [4], the plasma dynamics at a low current density had the following characteristic features.

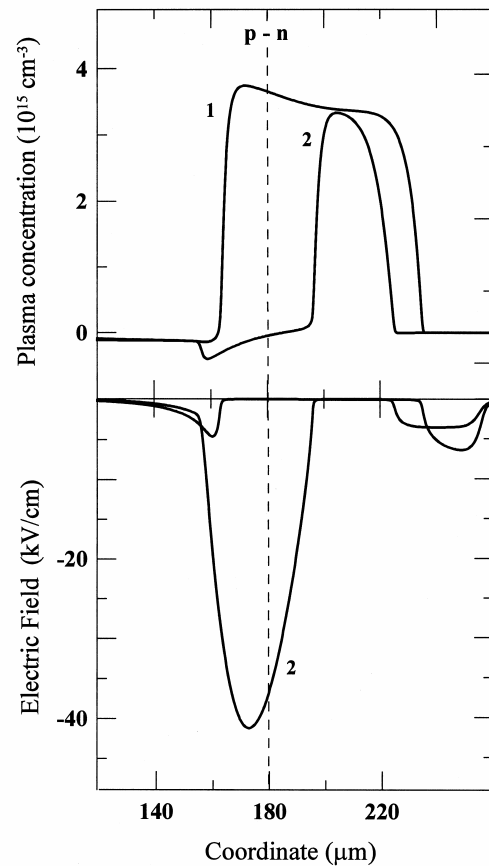


Fig.4. Distributions of the excess plasma concentration and electric field across the semiconductor structure upon the onset of current interruption (curve 1) and upon the time moment, at which the current dropped twice in amplitude (curves 2).

When the density of the forward pumping current was tens of A/cm^2 and the pumping time increased, the fraction of the charge accumulated in the p-region of the structure decreased. The reason was that at the stage of forward pumping the gradient of the charge-carrier concentrations near the p-n-junction increased as holes and electrons penetrated to the n- and p-region respectively. As a result, the diffusion current of charge carriers increased to a value of the order of

units of A/cm^2 . This value was comparable with the total current, leading to the change of the hole/electron current ratio near the p-n-junction (diffusion increased the hole current and decreased the electron current). As a result, the fraction of the accumulated charge decreased in the p-region and increased in the n-region. If the pumping time was made longer, the recombination loss in the p-region increased and, hence, the fraction of the charge accumulated in this region decreased still more.

The current cutoff stage had the following characteristic features. Similarly to the SOS effect regime at a high current density, before the commencement of the current cutoff process, the base and a portion of the p-region were filled with dense electron-hole plasma. Figure 4 presents the distribution of the excess plasma concentration in the structure (curve 1) for the current waveform in Fig. 2a at the moment the reverse current reached its maximum value. It is seen that the current cutoff process also started in the p-region of the structure. As the current decreased, mostly the left-hand boundary of the plasma moved towards the p-n-junction. The region of a strong field appeared in the structure, while the left-hand boundary crossed the p-n-junction and continued moving in the base. The distributions of the plasma concentration and the field in the structure (Fig. 4, curves 2) correspond to the moment of time, at which the current dropped twice and the output voltage at the structure and the load reached 65% of its maximum value.

Thus, the current cutoff stage is fully analogous to the corresponding stage in the SOS effect regime

when the current cutoff is due to the movement of the concentration front of dense excess plasma in the structure. A distinction is that this front crosses the p-n-junction during the current cutoff process. Although the current density is low ($100-150 A/cm^2$) during the current cutoff process, the switching process is sufficiently fast and takes a few nanoseconds. The reason is that a low current density is compensated by a small concentration of excess plasma on the front. Therefore, the front maintains its high speed at the stage of the current cutoff.

One more specific feature of the current cutoff process is related to a small magnitude of the electric field, which is formed in the structure. The reason is that the maximum of the region of the strong field is located in the p-region of the structure near the p-n-junction where the concentration of acceptors has a minimum value. The maximum field is about 40 kV/cm, while the total voltage of the structure is not higher than 250-300 V.

References

- [1] S.A. Darznez, S.K. Lyubutin, S.N. Rukin et al., *Elektrotehnika*, **4**, 20 (1999).
- [2] S.N. Rukin, *Instruments and Experimental Techniques*, **42**, 439 (1999).
- [3] S.N. Rukin, and S.N. Tsyranov, *Rus. J. Tech. Phys. Letters* **30**, No 1, 43 (2004).
- [4] S.A. Darznez, S.N. Rukin, and S.N. Tsyranov, *Rus. J. Tech. Physics* **45**, No 4, 436 (2000).